Journal of Non-Crystalline Solids 544 (2020) 120212

Contents lists available at ScienceDirect

Journal of Non-Crystalline Solids

journal homepage: www.elsevier.com/locate/jnoncrysol

# Chemical order in binary Se-Te glasses: Results from high-resolution 2D $^{77}$Se and $^{125}$Te MATPASS NMR spectroscopy

Bing Yuan[a], Ivan Hung[b], Zhehong Gan[b], Sabyasachi Sen[a,*]

[a] Department of Materials Science & Engineering, University of California at Davis, Davis, CA, 95616, USA
[b] Center of Interdisciplinary Magnetic Resonance, National High Magnetic Field Laboratory, 1800 East Paul Dirac Drive, Tallahassee, Florida, 32310, USA

ARTICLE INFO

*Keywords:*
Chalcogenide
Glass structure
2D NMR
Alloy
Selenium
Tellurium

ABSTRACT

The structure of binary $Te_xSe_{100-x}$ ($0 \leq x \leq 35$) glasses is studied using high-resolution two-dimensional magic-angle-turning phase-adjusted spinning sidebands (2D MATPASS) $^{77}$Se and $^{125}$Te nuclear magnetic resonance (NMR) spectroscopy. The $^{77}$Se ($^{125}$Te) isotropic NMR spectra are consistent with the presence of three different kinds of Se (Te) sites, which correspond to Se–**Se (Te)**–Se, Te–**Se (Te)**–Se, and Te–**Se (Te)**–Te environments. The compositional variation of the relative fractions of the three Se sites indicates that the Se and Te atoms are randomly distributed to form $[Se, Te]_n$ copolymer chains. The $^{77}$Se and $^{125}$Te NMR isotropic chemical shifts for Se and Te atoms in isostructural environments are found to display a linear correlation. The systematic compositional variation of the CSA of Se–**Se**–Se sites can be related to the appearance of Te atoms as next-nearest neighbors of Se atoms in the $[Se, Te]_n$ chains.

## 1. Introduction

Complex amorphous tellurides in the Ge-Sb-Te and related systems have found important technological applications in the areas of phase change memory and infrared photonics [1–3]. Recent studies have shown that $Te_xSe_{100-x}$ binary alloys can serve as a model system for the investigation of phenomena such as semiconductor-to-metal and reversible amorphous-to-crystalline transitions, which are relevant to phase-change memory applications [1]. Therefore, it is essential to study the structure of glasses in this system in order to understand the nature of these phase transitions for future applications.

Se and Te are isoelectronic and the structure of the stable crystalline polymorphs of both elements consists of polymeric $[Se]_n$ or $[Te]_n$ helical chains, where Se and Te atoms are twofold coordinated [4,5]. However, these two elements behave quite differently in their glass-forming tendencies. Se can be readily vitrified upon quenching of the parent melt, while Te can only be vitrified as thin films and readily crystallizes upon supercooling the melt in bulk. This difference between Se and Te limits the composition range for bulk glass formation in the $Te_xSe_{100-x}$ system to $x \leq 50$ [6,7]. The structure of $Te_xSe_{100-x}$ glasses have been studied in the past using a wide variety of techniques [8–10]. Although the atom rearrangement in these copolymer chains has been scrutinized using varies experimental techniques, no consensus has been reached yet. Itoh used a combination of neutron and X-ray diffraction and reverse Monte Carlo modeling and proposed a structural model for the $Te_{40}Se_{60}$ glass where Se and Te atoms are alternately connected with the presence of some $[Se]_n$ fractions and Te-Te dimers in $[Se, Te]_n$ chains [8]. On the other hand, a recent Raman spectroscopic study suggested that the Se and Te atoms are randomly distributed in the copolymeric $[Se, Te]_n$ chains with some preference for heteropolar bonding [9]. This structural model is similar to that originally proposed by Bureau et al. [10] on the basis of a $^{77}$Se magic-angle spinning (MAS) nuclear magnetic resonance (NMR) spectroscopic study. These authors reported the composition dependent variation of the relative fraction of different Se environments as obtained from the simulation of the $^{77}$Se MAS NMR spectral line shapes. However, the experimental conditions utilized by these authors ($^{77}$Se resonance frequency of 57.3 MHz and spinning speed of 15 kHz) precluded complete separation of spinning sidebands from isotropic peaks due to the relatively large chemical shift anisotropy (CSA) and chemical shift distribution for $^{77}$Se that are characteristic of the constituent Se environments. These authors also reported the $^{125}$Te MAS NMR spectra of these glasses, although the CSA and chemical shift distribution related line broadening was found to be too large for $^{125}$Te to retrieve any information regarding Te speciation [10].

$^{77}$Se and $^{125}$Te NMR spectroscopy remain challenging in chalcogenide glasses due to the low natural abundance of these nuclides (~7% each), their long spin-lattice relaxation times, large CSA and chemical

---

* Corresponding author.
*E-mail address:* sbsen@ucdavis.edu (S. Sen).

https://doi.org/10.1016/j.jnoncrysol.2020.120212
Received 30 April 2020; Received in revised form 1 June 2020; Accepted 3 June 2020

shift range, which are particularly problematic for $^{125}$Te. These issues result in lengthy data collection and broad and unresolved NMR spectra. Some of these problems can be alleviated effectively via the implementation of the two-dimensional magic-angle turning phase-adjusted spinning sidebands (2D MATPASS) NMR technique. The MATPASS technique can separate the CSA from the isotropic chemical shift, resulting in increased spectral resolution in the isotropic dimension, while preserving the information contained in the CSA along the anisotropic dimension [11]. This separation of isotropic and anisotropic chemical shift interactions results in an isotropic NMR spectrum corresponding to a high-resolution MAS spectrum at infinite spinning speed, i.e., free of any CSA-related broadening. Moreover, a consideration of CSA in combination with isotropic shift can often provide unequivocal identification of structural units. The isotropic vs anisotropic separation experiment allows the use of high magnetic fields for increased sensitivity and resolution without requiring faster spinning with small sample volume rotors. Finally, the application of the Carr-Purcell Meiboom-Gill (CPMG) echo train acquisition of the MATPASS data can reduce the data collection time significantly [11]. In this work, we report the results of a combined high-resolution $^{77}$Se and $^{125}$Te 2D MATPASS/CPMG NMR spectroscopic study of the structure and chemical order in binary $Te_xSe_{100-x}$ glasses with $0 \leq x \leq 35$. The compositional evolution of the relative fractions of different Se and Te environments as obtained from the corresponding isotropic NMR spectra provides unique information on the bonding preference of Se and Te atoms in these glasses. Additionally, the CSA of the Se sites, as obtained from the anisotropic spectra, reveals the effect of the replacement of Se next-nearest neighbors with Te.

## 2. Experimental

### 2.1. Sample synthesis and physical characterization

Binary $Te_xSe_{100-x}$ glasses with $x = 0, 10, 20, 25, 30, 35$ were synthesized in ~14 g batches from mixtures of constituent elements (Alfa Aesar, 99.999%) that were taken in evacuated fused quartz ampoules and melted at 873 K for 12 h. The melts were then quenched by dipping the ampoules in ice-water. Chemical analysis of all glasses was carried out using an electron microprobe (Cameca SE-100) equipped with wavelength dispersive spectrometers. The compositions of all glasses were found to be within ± 0.5 at% of nominal and they were chemically homogeneous at the micron-scale.

The density of these $Te_xSe_{100-x}$ glasses was measured using a Micrometritic Accupyc II gas expansion pycnometer under helium (6 N purity) environment. For each measurement, approximately 1.0 g of glass sample was loaded into a 1 cm$^3$ cup. The reported densities in this study are averages of 10 consecutive measurements at room temperature.

### 2.2. NMR spectroscopy

The 2D $^{77}$Se and $^{125}$Te MATPASS/CPMG NMR spectra for all glasses were acquired at the National High Magnetic Field Laboratory using a 31 mm bore 19.6T magnet equipped with a Bruker Avance NEO console operating at the resonance frequency of 158.7 MHz and 262.3 MHz for $^{77}$Se and $^{125}$Te, respectively. Glass samples were crushed and packed into 3.2 mm $ZrO_2$ rotors and were spun at 10 kHz.

The MAT/CPMG pulse sequence [11] was used for $^{77}$Se with $\pi/2$ and $\pi$ pulses of 3.0 and 6.0 μs, respectively. The method of States et al. [12] for hypercomplex data acquisition was applied to the CPMG pulse phase and the receiver phase. The 2D acquisition consisted of 16 hypercomplex $t_1$ increments each with 36 transients, 81 CPMG echoes per transient and 75 s recycle delay, for a total experimental duration of 24 h per spectrum. For $^{125}$Te, the projection version of the pulse sequence, *pj*MAT/CPMG [13], was used for covering the wider $^{125}$Te frequency range with all pulses set to 2.7 μs. The 2D acquisition consisted of 16 hypercomplex $t_1$ increments spanning only half a rotor period ($-\tau_r/4$ to $+\tau_r/4$), each with 360 transients, 13 CPMG echoes per transient and 30 s recycle delay, for a total experimental duration of 96 h per spectrum. The 2D MAT spectra were sheared to an isotropic/anisotropic representation in the direct/indirect dimensions during processing, as detailed in Ref. [11]. The isotropic and anisotropic line shapes were simulated using DMFit [14]. $^{77}$Se and $^{125}$Te NMR spectra were externally referenced by recording the $^{17}$O signal of natural abundance $H_2O$ and using the appropriate frequency ratios reported in the IUPAC recommendations [15]. The chemical shift anisotropy (CSA) tensors reported here are defined using the Haeberlen convention [16] as:

$$|\delta_{zz} - \delta_{\mathrm{iso}}| \geq |\delta_{xx} - \delta_{\mathrm{iso}}| \geq |\delta_{yy} - \delta_{\mathrm{iso}}|,$$

$$\delta_{\mathrm{iso}} = \frac{1}{3}(\delta_{zz} + \delta_{xx} + \delta_{yy}),$$

$$\Delta = \delta_{zz} - \delta_{\mathrm{iso}},$$

$$\eta = \frac{\delta_{yy} - \delta_{xx}}{\Delta},$$

where $\delta_{xx}$, $\delta_{yy}$, and $\delta_{zz}$ are the principle components of the chemical shift tensor and $\delta_{\mathrm{iso}}$ is the isotropic chemical shift. The magnitude of the CSA is $\Delta$, and the asymmetry of the CSA is denoted by $\eta$.

## 3. Results and discussion

$^{77}$Se isotropic NMR spectra of the $Te_xSe_{100-x}$ ($x$ = 0 - 35) glasses are shown in Fig. 1. The $^{77}$Se NMR spectrum of glassy Se shows a single symmetric broad peak with $\delta_{\mathrm{iso}} \sim 870$ ppm, which can be unambiguously assigned to a Se–**Se**–Se environment [17,18]. The initial addition of Te gives rise to a new Se environment, which appears as a shoulder centered near $\delta_{\mathrm{iso}} \sim 750$ ppm. Progressive increase in the Te content results in an increase in the intensity of this shoulder as well as the appearance of a low-frequency tail centered near $\delta_{\mathrm{iso}} \sim 600$ ppm, which becomes prominent in Te-rich compositions ($x \geq 30$). These two isotropic $^{77}$Se resonances can be assigned on the basis of a previous study by Bureau et al. [10] to Se–**Se**–Te and Te–**Se**–Te environments, respectively. Accordingly, the $^{77}$Se isotropic NMR spectra were fitted with three Gaussian peaks to obtain the composition-dependent variation of the relative fractions for the three Se environments (Fig. 1). The intensity, position and width of these peaks corresponding to the best fits are listed in Table 1. The $\delta_{\mathrm{iso}}$ for these Se environments display a nearly linear shift to lower frequency by ~ 100 ppm with the replacement of each Se nearest neighbor by a Te atom (Table 1). This trend and the absolute values of $^{77}$Se $\delta_{\mathrm{iso}}$ are in qualitative agreement with those reported in previous $^{77}$Se MAS NMR studies of binary Se-Te and ternary Ge-Se-Te glasses as well as with the density functional theory (DFT) based calculations of $^{77}$Se NMR $\delta_{\mathrm{iso}}$ of these Se environments in short Se-Te chain segments terminated by H atoms [10,19]. This trend was attributed in a previous study [19] to the increased shielding at the central Se site as the more electronegative Se atom pulls the large electron cloud from the nearest neighbor Te atoms towards itself. The relative area fractions of these three peaks yield the compositional evolution of the relative fractions of the Se–**Se**–Se, Se–**Se**–Te and Te–**Se**–Te Se environments (Table 1). This variation is shown in Fig. 2 and is compared to two different structural models, namely the chain crossing model and the random distribution model, to elucidate the bonding preference between Se and Te atoms in these glasses.

The chain crossing model assumes a perfectly homogeneous distribution of the Te atoms in the $[Se,Te]_n$ copolymeric chains such that the Te atoms are all separated by equal distance. On the other hand, the random distribution model assumes a random spatial distribution of Te atoms in the $[Se,Te]_n$ copolymeric chains such that there is no preference between the formation of heteropolar and homopolar bonds for either Se or Te [10]. It is clear from Fig. 2 that the Se site speciation in

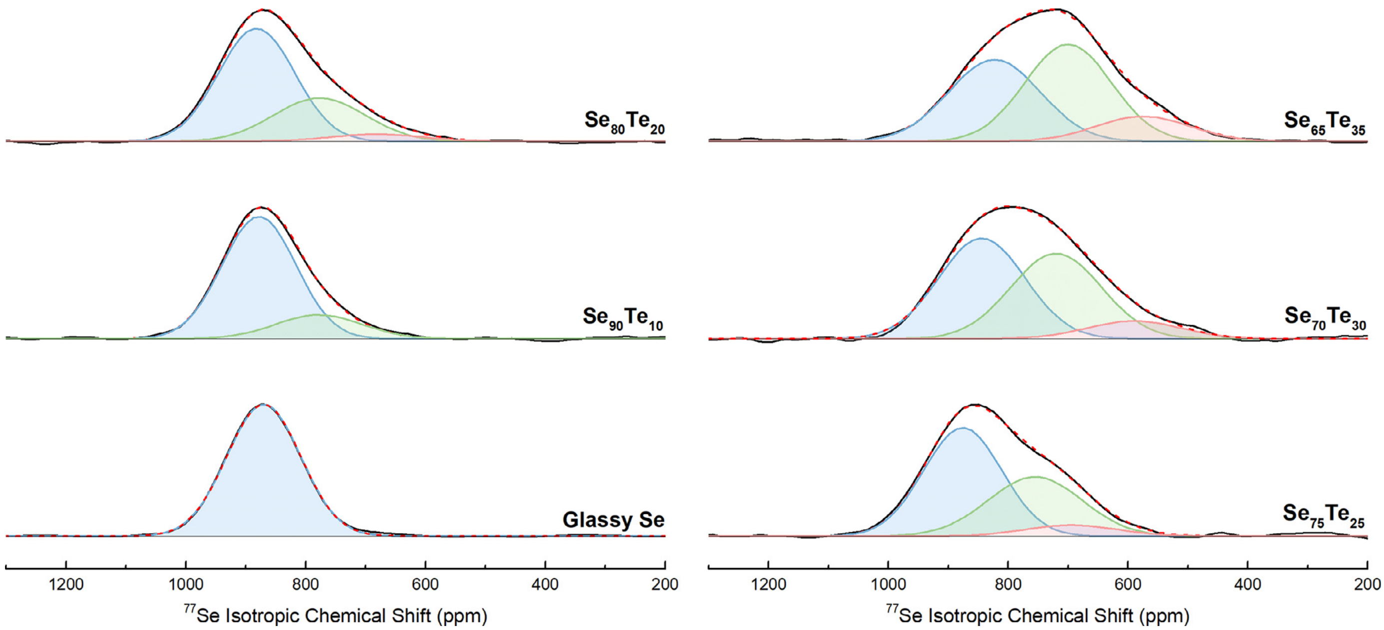

**Fig. 1.** Experimental (black solid lines) and simulated (red dashed lines) $^{77}$Se isotropic NMR spectra for $Te_xSe_{100-x}$ glasses. Individual simulation components for Se–**Se**–Se, Se–**Se**–Te and Te–**Se**–Te sites are denoted in blue, green and pink, respectively. (For interpretation of the references to color in this figure legend, the reader is referred to the web version of this article.).

these $Te_xSe_{100-x}$ glasses shows remarkable agreement with that expected from the random distribution model, which suggests an equal preference for Se (Te) atoms to form Se–Se (Te–Te) and Se–Te bonds. This result is in qualitative agreement with previous Raman and $^{77}$Se MAS NMR spectroscopic studies that suggest a nearly random distribution of Se and Te atoms in the structure of these glasses [9,10]. However, it may be noted that these previous studies indicated some preference for heteropolar bonding, while the Se speciation results obtained in the present study suggest a perfectly random distribution within experimental error.

The $^{125}$Te isotropic NMR spectra of $Te_xSe_{100-x}$ glasses with $25 \leq x \leq 35$ are shown in Fig. 3. The short $T_2$ relaxation time of $^{125}$Te makes it practically impossible to obtain $^{125}$Te MATPASS NMR spectra of glasses with $x \leq 25$. It is clear that compared to the $^{77}$Se isotropic NMR spectra in Fig. 1 the $^{125}$Te spectral line shapes display poorer resolution and signal:noise ratio as the latter are severely broadened by the large chemical shift distribution that is characteristic of the $^{125}$Te nuclide. However, similar to Se, one expects the Te atoms to be present in three different environments, namely Se–**Te**–Se, Te–**Te**–Se, and Te–**Te**–Te, consistent with the observation that none of the $^{125}$Te isotropic NMR line shapes can be fitted well with a single Gaussian peak. Although attempts at simulation of these line shapes with three peaks corresponding to the three Te environments did not lead to unique solutions, the peak positions appear to be invariably located near $\delta_{iso} \sim$ 1100, 1300 and 1500 ppm. Previous $^{125}$Te *pj*MATPASS/CPMG NMR studies of As-Te glasses suggest that the lowest frequency peak near 1100 ppm corresponds to the Te–**Te**–Te environment [13]. Consequently, the $^{125}$Te $\delta_{iso}$ at ~ 1300 and 1500 ppm can be assigned to the Te–**Te**–Se and Se–**Te**–Se environments (Fig. 3). An example of such a fit is shown in Fig. 3 where the relative areas of the three peaks were constrained to remain close to the expected random distribution. Despite the lower signal:noise ratio relative to the $^{77}$Se spectra, the compositional evolution of the $^{125}$Te isotropic NMR spectral line shapes is thus consistent with a random distribution of Te atoms in the glass structure. It is interesting to note here that the $^{77}$Se and $^{125}$Te $\delta_{iso}$ for the isostructural nearest-neighbor environments of Se and Te atoms are approximately linearly correlated according to the relation: $\delta_{iso}(^{125}Te)_{ppm} = 1.75^* \delta_{iso}(^{77}Se)_{ppm}$. Such linear relationships were also reported in previous NMR studies of organoselenium and organotellurium compounds as well as of polychalcogenide anions [20].

The molar volume of these $Te_xSe_{100-x}$ glasses displays a linear increase with increasing Te content (Fig. 4). An extrapolation of this trend to pure Te shows good agreement with the experimental molar volume of amorphous Te film, as reported in a previous study by Ichikawa [21]. This molar volume trend of $Te_xSe_{100-x}$ glasses is nearly parallel with that of crystalline $Te_xSe_{100-x}$ solid solutions [22]. X-ray diffraction

**Table 1**
Simulation parameters for $^{77}$Se isotropic NMR line shapes.

| Glass composition | Se | $Te_{10}Se_{90}$ | $Te_{20}Se_{80}$ | $Te_{25}Se_{75}$ | $Te_{30}Se_{70}$ | $Te_{35}Se_{65}$ |
|---|---|---|---|---|---|---|
| Se–**Se**–Se | | | | | | |
| $\delta_{iso}$( ± 10 ppm) | 869 | 878 | 882 | 876 | 844 | 826 |
| peak width ( ± 10 ppm) | 145 | 145 | 150 | 154 | 170 | 165 |
| relative fraction ( ± 5%) | 100 | 81 | 65 | 56 | 48 | 39 |
| Te–**Se**–Se | | | | | | |
| $\delta_{iso}$( ± 10 ppm) | | 778 | 777 | 755 | 720 | 700 |
| peak width ( ± 10 ppm) | | 170 | 180 | 185 | 178 | 170 |
| relative fraction ( ± 5%) | | 19 | 30 | 37 | 43 | 49 |
| Te–**Se**–Te | | | | | | |
| $\delta_{iso}$( ± 10 ppm) | | | 680 | 694 | 590 | 570 |
| peak width ( ± 10 ppm) | | | 185 | 183 | 185 | 177 |
| relative fraction ( ± 5%) | | | 5 | 7 | 9 | 12 |

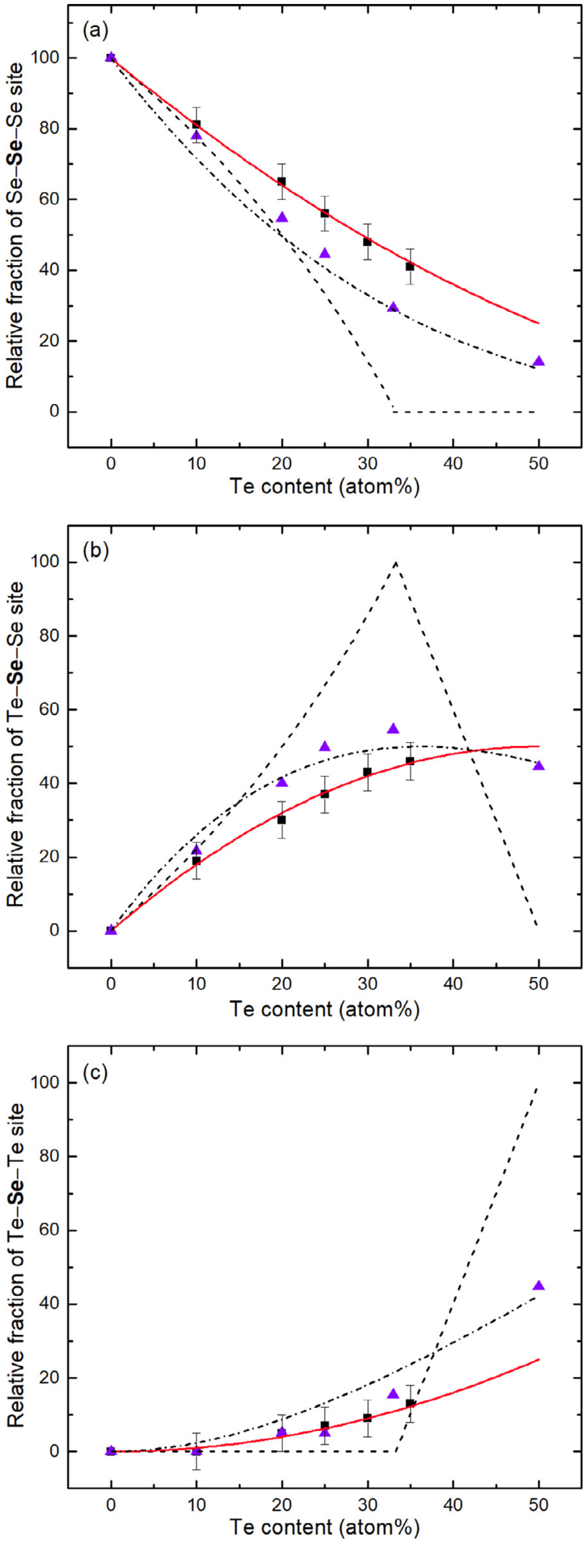

**Fig. 2.** Compositional variation of (a) Se–**Se**–Se, (b) Se–**Se**–Te and (c) Te–**Se**–Te site fractions obtained from simulations of $^{77}$Se isotropic NMR spectra (black squares). Literature values from a previous $^{77}$Se MAS NMR spectroscopic study (purple triangles) [10], chain crossing model (dashed black line), random distribution model (solid red line), and partially random distribution model with some preference for heteropolar bonding as reported in [10] (dashed dotted black line). Solid triangles are data from [10] as determined from $^{77}$Se MAS NMR spectra. (For interpretation of the references to color in this figure legend, the reader is referred to the web version of this article.).

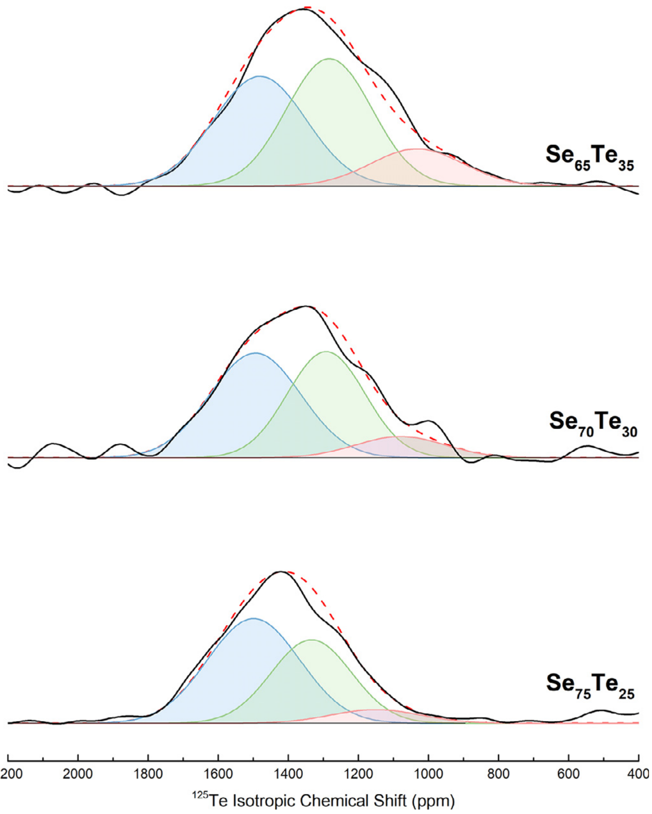

**Fig. 3.** Experimental (black solid lines) and simulated (orange dashed lines) $^{125}$Te isotropic NMR spectra for $Te_xSe_{100-x}$ glasses. Individual simulation components for Se–**Te**–Se, Se–**Te**–Te and Te–**Te**–Te sites are denoted in blue, green and pink, respectively. (For interpretation of the references to color in this figure legend, the reader is referred to the web version of this article.).

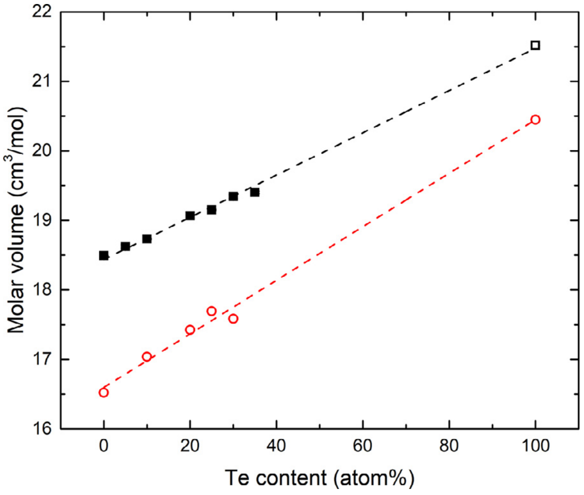

**Fig. 4.** Molar volume of $Te_xSe_{100-x}$ bulk glasses (filled squares) and crystals (open circles). Straight lines represent the linear least squares fit to the experimental data. The molar volume for amorphous Te film (open square) is from [21], while the data for the crystals are from [22].

analysis of these crystalline alloys have been shown to be consistent with Se and Te atoms forming copolymeric $[Se,Te]_n$ chains [23]. Therefore, the similar linear compositional variation of the molar volumes of $Te_xSe_{100-x}$ glasses in Fig. 4 may be interpreted to be indicative of the presence of similar $[Se,Te]_n$ chains in the amorphous state. This structural scenario is in clear agreement with the NMR results discussed above.

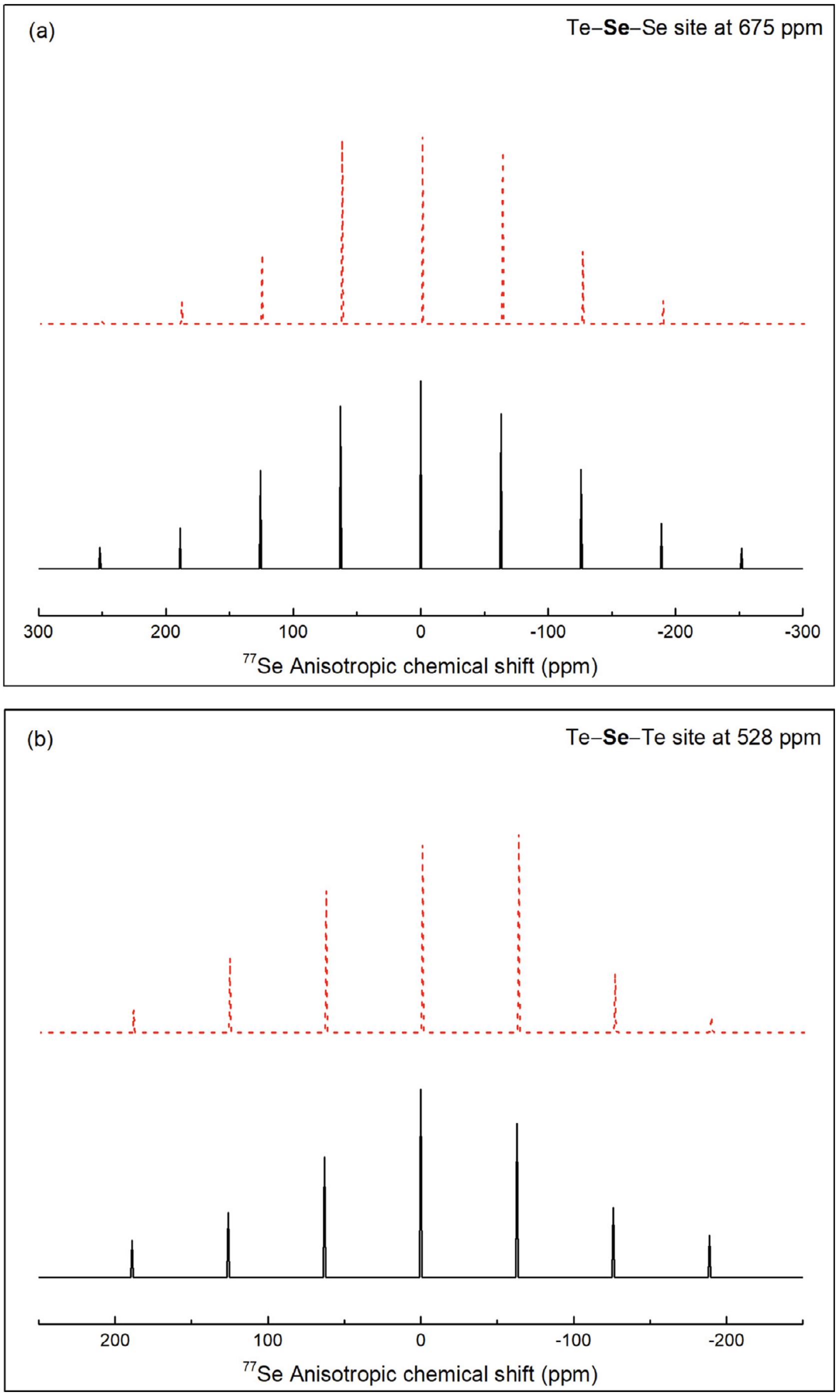

**Fig. 5.** Representative experimental $^{77}$Se NMR anisotropic spinning sideband intensities (solid lines) for (a) Se–**Se**–Te and (b) Te–**Se**–Te sites in $Te_xSe_{100\text{-}x}$ glasses. Anisotropic slices for these three sites are taken at $\delta_{iso}$ = 675 and 528 ppm, respectively. Corresponding simulations are shown as dashed lines.

Further insights into the bonding environments in these glasses can be obtained from a consideration of the CSA parameters. Unfortunately, Δ and $\eta$ for the different Se and Te sites cannot be readily isolated due to substantial overlap of the isotropic resonances for the different environments, which is particularly severe for the $^{125}$Te spectral line shapes (Fig. 3). However, for the $^{77}$Se NMR spectra, we have analyzed the anisotropic spectral slices taken at the $\delta_{iso}$ for the Se-**Se**-Te and Te-**Se**-Te sites where the overlap from the neighboring peaks is minimal. The spinning sideband intensities of these anisotropic spectra and their simulations are shown in Fig. 5. The average $\eta$ for the Se–**Se**–Te and Te–**Se**–Te sites do not show significant variation and vary between and 0.75 to 0.90. However, the Δ for these two sites (−180 ppm) is significantly higher than that (−150 ppm) reported in a previous study [18] for the Se-**Se**-Se site in glassy Se. Moreover, the Δ values for the Se-**Se**-Se sites decreases systematically from −150 to −170 ppm as $\delta_{iso}$ decreases from ~ 880 to 825 ppm, with increasing Te content (Fig. 6). It is interesting to note that similar trends were also reported in the literature for the Ge-Se system and were ascribed to the replacement of Se with Ge as next-nearest neighbors with progressive addition of Ge [24]. Therefore, it is tempting to speculate that Te has a similar effect on the Δ and $\delta_{iso}$ of the Se nuclides in the Se–**Se**–Se sites. This hypothesis is indeed consistent with the DFT based calculations reported in a previous study that indicated a lowering of the $^{77}$Se $\delta_{iso}$ of the Se-**Se**-Se site by 30 ppm as a Se next-nearest neighbor is replaced by a Te

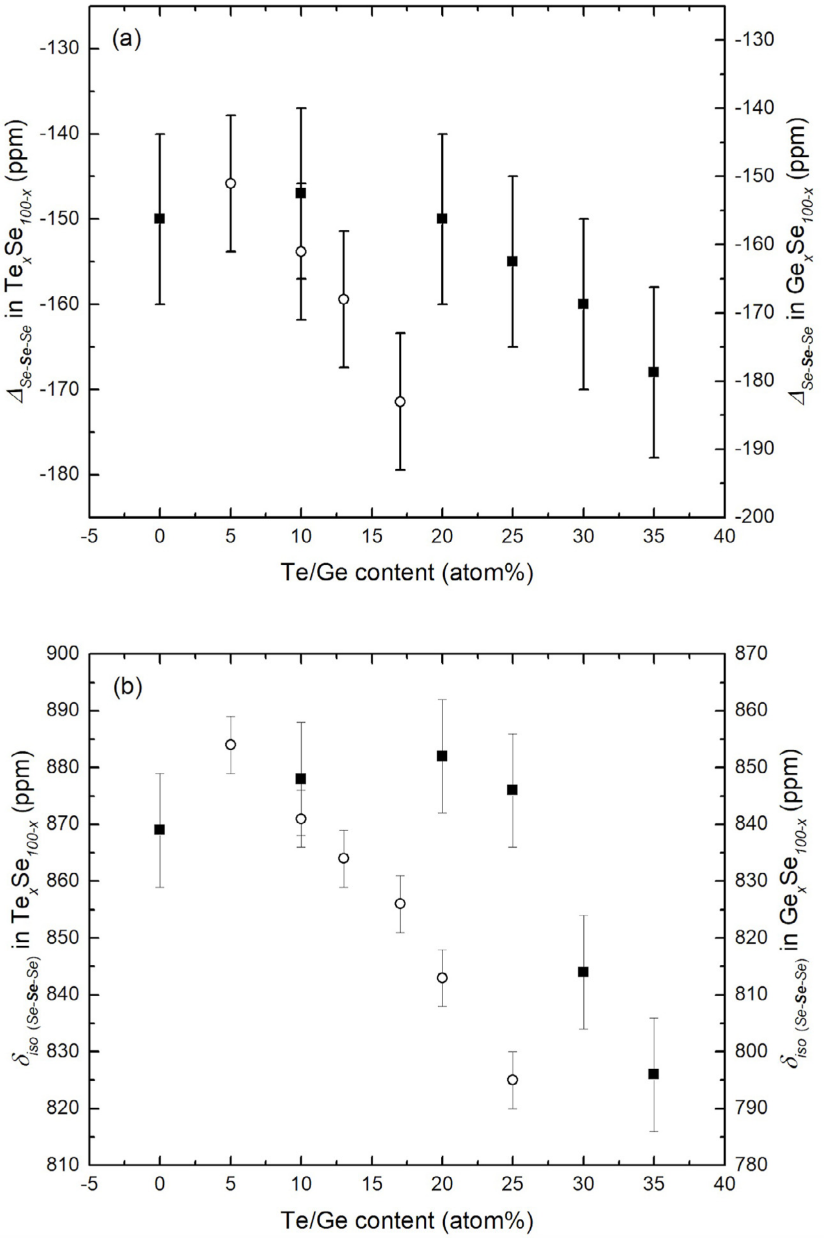

**Fig. 6.** Compositional variation of average $^{77}$Se (a) $\Delta$ and (b) $\delta_{iso}$ for Se–**Se**–Se sites in $Te_xSe_{100-x}$ glasses (filled squares). Corresponding variation in $Ge_xSe_{100-x}$ glasses (open circles), taken from a previous study [24] is shown for comparison.

atom [19].

## 4. Summary

$^{77}$Se and $^{125}$Te 2D MATPASS/CPMG NMR spectroscopy can provide increased site resolution by separating and correlating the isotropic and the anisotropic chemical shift in two dimensions. The $^{77}$Se isotropic NMR spectra allows for the identification of three different Se environments, namely Se–**Se**–Se, Se–**Se**–Te and Te–**Se**–Te sites. The compositional variation of the relative fractions of these sites suggest a completely random distribution of Se and Te atoms in $[Se,Te]_n$ copolymeric chains. Such finding is also consistent with the compositional variation of the molar volumes of these glasses. Moreover, the $^{125}$Te isotropic NMR spectral line shapes can be reconstructed by three different Te sites, namely Te–**Te**–Te, Te–**Te**–Se and Se–**Te**–Se sites, with consistent $\delta_{iso}$ and peak area ratios constrained by the random distribution model, which indirectly confirms the $^{77}$Se NMR results. Further insights into the local bonding environments are provided by the $^{77}$Se CSA parameters of all Se sites. The $^{77}$Se ($^{125}$Te) $\delta_{iso}$ values vary linearly with the number of nearest-neighbor Te (Se) atoms. Additionally, the $^{77}$Se and $^{125}$Te $\delta_{iso}$ for isostructural nearest-neighbor environments of Se and Te atoms are found to be linearly correlated. The systematic dependence of $\Delta$ and $\delta_{iso}$ of the Se–**Se**–Se site with Te concentration can be attributed to the appearance of Te atoms as next-nearest neighbors.

## Declaration of Competing Interest

The authors declare that they have no known competing financial interests or personal relationships that could have appeared to influence the work reported in this paper.

## Credit author statement

**Bing Yuan**: Glass synthesis, molar volume measurements, NMR data processing and interpretation, writing of manuscript. **Sabyasachi Sen**: Conceived the project, provided supervision and help with data interpretation and writing of the manuscript. **Ivan Hung** and **Zhehong Gan:** contributed equally to the design and implementation of NMR spectroscopic technique, NMR data collection, and reviewing and editing of the manuscript.

## Acknowledgment

This study is supported by the National Science Foundation Grant NSF-DMR 1855176. Part of this work was supported by the National High Magnetic Field Laboratory (NHMFL) in Tallahassee, FL, USA, through NSF DMR-1644779 and the State of Florida.

## References

[1] P.A. Vermeulen, J. Momand, B.J. Kooi, Reversible amorphous-crystalline phase changes in a wide range of $Se_{1-x}Te_x$ alloys studied using ultrafast differential scanning calorimetry, J. Chem. Phys. 141 (2014) 024502.

[2] M. Wuttig, N. Yamada, Phase-change materials for rewriteable data storage, Nat. Mater. 6 (2007) 824.

[3] B. Bureau, X.H. Zhang, F. Smektala, J.L. Adam, J. Troles, H.L. Ma, C. Boussard-Plèdel, J. Lucas, P. Lucas, D. Le Coq, M.R. Riley, J.H. Simmons, Recent advances in chalcogenide glasses, J. Non. Cryst. Solids. 345&346 (2004) 276–283.

[4] G. Lucovsky, A. Mooradian, W. Taylor, G.B. Wright, R.C. Keezer, Identification of the fundamental vibrational modes of trigonal, α-monoclinic and amorphous selenium, Solid State Commun. 5 (1967) 113–117.

[5] E. Grison, Studies on tellurium-selenium alloys, J. Chem. Phys. 19 (1951) 1109–1113.

[6] A. Zakery, S.R. Elliott, Optical properties and applications of chalcogenide glasses: a review, J. Non. Cryst. Solids. 330 (2003) 1–12.

[7] M. Popescu, Non-Crystalline Chalcogenides, Kluwer Academic Publishers, 2002.

[8] K. Itoh, Structure of Se-Te glasses studied using neutron, X-ray diffraction and reverse Monte Carlo modelling, J. Solid State Chem. 246 (2017) 372–378.

[9] A. Tverjanovich, A. Cuisset, D. Fontanari, E. Bychkov, Structure of Se-Te glasses by Raman spectroscopy and DFT modeling, J. Am. Ceram. Soc. 101 (2018) 5188–5197.

[10] B. Bureau, C. Boussard-plèdel, M. Lefloch, J. Troles, J. Lucas, D. Rennes, D. Beaulieu, Selenium-tellurium sequences in binary glasses as depicted by $^{77}$Se and $^{125}$Te NMR, J. Phys. Chem. B. 109 (2005) 6130–6135.

[11] I. Hung, T. Edwards, S. Sen, Z. Gan, MATPASS/CPMG: a sensitivity enhanced magic-angle spinning sideband separation experiment for disordered solids, J. Magn. Reson. 221 (2012) 103–109.

[12] D.J. States, R.A. Haberkorn, D.J. Ruben, A 2D Nuclear Overhauser Experiment with pure absorption phase in four quadrants, J. Magn. Reson. 48 (1982) 286–292.

[13] D.C. Kaseman, I. Hung, K. Lee, K. Kovnir, Z. Gan, B. Aitken, S. Sen, Tellurium speciation, connectivity, and chemical order in $As_xTe_{100-x}$ glasses: results from two-dimensional $^{125}$Te NMR spectroscopy, J. Phys. Chem. B. 119 (2015) 2081–2088.

[14] D. Massiot, F. Fayon, M. Capron, I. King, S. Le Calvé, B. Alonso, J.O. Durand, B. Bujoli, Z. Gan, G. Hoatson, Modelling one- and two-dimensional solid-state NMR spectra, Magn. Reson. Chem. 40 (2002) 70–76.

[15] R.K. Harris, E.D. Becker, S.M. Cabral De Menezes, R. Goodfellow, P. Granger, NMR nomenclature: nuclear spin properties and conventions for chemical shifts (IUPAC recommendations 2001), Pure Appl. Chem. 73 (2001) 1795–1818.

[16] U. Haeberlen, High Resolution NMR in Solids Selective Averaging: Supplement 1 Advances in Magnetic Resonance, Elsevier, 2012.

[17] B. Bureau, J. Troles, M. Le Floch, F. Smektala, J. Lucas, Medium range order studied in selenide glasses by $^{77}$Se NMR, J. Non. Cryst. Solids. 326&327 (2003) 58–63.

[18] M. Marple, J. Badger, I. Hung, Z. Gan, K. Kovnir, S. Sen, Structure of amorphous selenium by 2D $^{77}$Se NMR spectroscopy: an end to the dilemma of chain versus ring, Angew. Chemie. 129 (2017) 9909–9913.

[19] L. Bouëssel Du Bourg, C. Roiland, L. Le Pollès, M. Deschamps, C. Boussard-Plédel, B. Bureau, C.J. Pickard, E. Furet, Impact of Te on the structure and $^{77}$Se NMR spectra of Se-rich Ge-Te-Se glasses: a combined experimental and computational investigation, Phys. Chem. Chem. Phys. 17 (2015) 29020–29026.

[20] M. Björgvinsson, G.J. Schrobilgen, Homo-and Heteropolychalcogenide Anions Ch HCh, Ch, Ch and $Ch^{2-}$ (Ch = Se and/or Te): solution $^{1}$H, $^{77}$Se, $^{123}$Te, and $^{125}$Te NMR study, Inorg. Chem. 30 (1991) 2540–2547.

[21] T. Ichikawa, Electron diffraction study of the local atomic arrangement in amorphous tellurium films, Phys. Stat. Sol. (B) 56 (1973) 707–715.

[22] G.C. Das, M.B. Bever, D.R. Uhlmann, S.C. Moss, Relaxation phenomena in selenium-tellurium alloys, J. Non. Cryst. Solids. 7 (1972) 251–270.

[23] E. Grison, Studies on tellurium-selenium alloys, J. Chem. Phys. 19 (1951) 1109–1113.

[24] D.C. Kaseman, I. Hung, Z. Gan, S. Sen, Observation of a continuous random network structure in $Ge_xSe_{100-x}$ glasses: results from high-resolution $^{77}$Se MATPASS/CPMG NMR spectroscopy, J. Phys. Chem. B. 117 (2013) 949–954.